Cortical Microstructure from Diffusion MRI Improves Tau PET Prediction Beyond Plasma pTau217 and Macrostructural Atrophy

Ritobrato Datta[1], Gerard Ridgway[2], Mario Torso[2], Pegah Khosropanah[2], Gayle Wittenberg[3], Steven A. Chance[2], Ziad S. Saad[1]

AFFILIATIONS: [1]Johnson and Johnson, La Jolla, CA, USA, [2]Oxford Brain Diagnostics, Oxford, United Kingdom, [3]Johnson and Johnson, Titusville, NJ, USA.

Key takeaway

Diffusion MRI–derived cortical microstructure (CDM PerpPD⁺) strongly associates with regional tau PET and adds complementary predictive power beyond plasma pTau217 and macrostructural atrophy.

Background

- The Alzheimer's disease cascade is thought to involve an amyloid-induced spread of tau from the medial temporal lobe to the neocortex (Sanchez, 2021; PMID:33472953).
- Tau pathology assessed in vivo with PET shows strong temporal and spatial associations with subsequent longitudinal atrophy patterns and their clinical correlates (La Joie, 2020; PMID:31894103).
- Microstructural changes are understood to precede macrostructural atrophy (Weston, 2015; PMID:26136857), motivating assessment of the associations of tau PET with microstructural measures from diffusion MRI.

Methods

- 101 subjects from the ADNI database were selected based on the inclusion-exclusion criteria for the Autonomy trial (Henley CTAD2024).

	CN	MCI	AD
Exc.Low	22	16	
Inc.Low	23	28	1
Inc.High	0	7	0
Exc.High	0	0	4
	45	51	5

- Demographics
  - 55 male, 46 female; Age (mean ± SD) 75.4 ± 7.7 yrs, median 75.8, range 57.9 – 91.4 yrs; APOE e4 count (0 - 35; 1 – 50; 2 – 16)
- Assessments
  - MMSE (mean ± SD) 27.5 ± 2.9 points, median 28, range 11 to 30; CDR-SB (mean ± SD) 1.3 ± 2.0 points, median 0.5, range 0 to 11; CDR global 0.3 ± 0.3, median 0.5, range 0 to 2
  - Plasma pTau217 and tauPET were collected within ±100 days of an MRI scan including diffusion MRI (min. directions = 30)
- Cortical Disarray Measurement (CDM) from Oxford Brain Diagnostics Ltd. provides minicolumn-associated cortical microstructure measurements of neurodegeneration from each individual timepoint (Torso, 2022).
  - CDM measures have been validated against Braak staging and against post-mortem ground truth (Torso, 2023; PMID: 37794477) and are associated with Synaptic biomarker CSF GAP-43 (ADPD 2023)

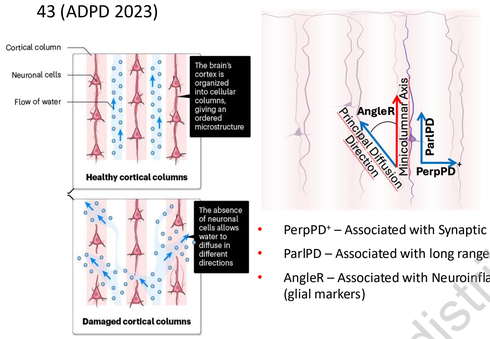

- PerpPD⁺ – Associated with Synaptic density
- ParlPD – Associated with long range projections
- AngleR – Associated with Neuroinflammation (glial markers)

PerpPD⁺ (Torso, 2022) measures were averaged across Desikan-Killiany regions and an AD-signature meta-region (Ridgway CTAD2022, Torso 2025; PMID:40420356). TauPET SUVR was generated using in house methods (Saad 2026) averaged over an inferior temporal region (inftemp) and a Braak-IV meta-region (Therriault, 2022). PerpPD⁺ was adjusted for scanner model and dMRI protocol.

Results

Figure1A: Progressive Elevation of different biomarkers from imaging and plasma across Diagnostic Stages

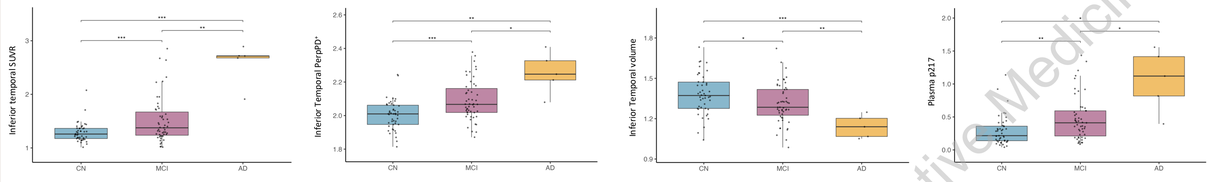

Figure1B: Progressive Elevation of different biomarkers from imaging and plasma across Diagnostic Stages and Tau-Stratified Groups

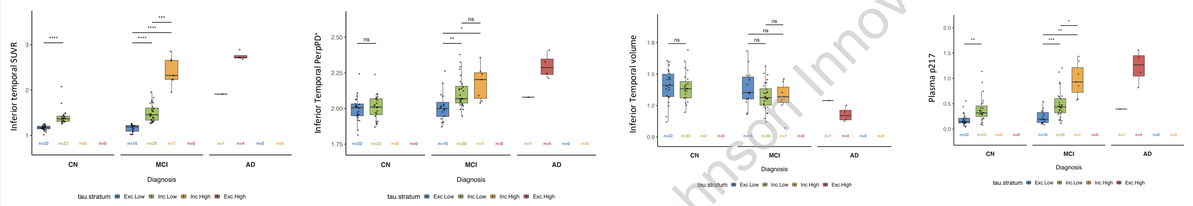

- The different imaging measures and plasma p217 levels show a stepwise increase from CN → MCI → AD, with AD highest and statistically higher than both CN and MCI, while MCI is also higher than CN (Figure 1A)
- Within each diagnosis group, plasma pTau217 tends to increase with higher tau strata, with clear elevation from Exc.Low to Inc.Low/Inc.High/Exc.High, especially in MCI and AD; however, AD strata have very small sample sizes warranting cautious interpretation (Fig. 1B)

Figure 2: Inferior Temporal Tau PET SUVR vs CDM PerpPD⁺

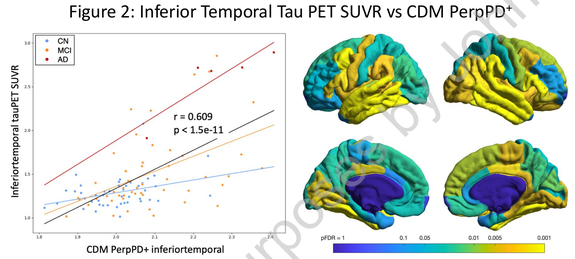

- Inftemp TauPET shows high correlation with inftemp PerpPD⁺ (r = 0.61, Figure 2, left) and with PerpPD⁺ across predominantly temporal regions (right).

Figure 3: Braak 4 Tau PET SUVR vs CDM PerpPD⁺

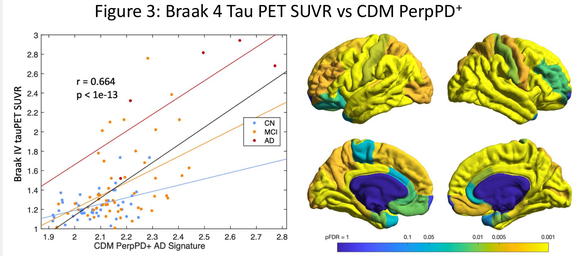

- TauPET in Braak-IV showed stronger (r = 0.66, Figure 3, left) correlation with PerpPD⁺ in AD-signature region and more spatially extended correlations across the brain (right).

Table 1: Model Comparison to predict taupet

Inferior Temporal TauPET			
Predictors	Adj_R^2	F_stat	p_value
pTau217	0.63	172.25	2.14E-23
pTau217 + sex	0.63	0.04	8.38E-01
pTau217 + sex + age	0.64	3.83	5.33E-02
pTau217 + sex + age + InfTemp cortical thickness	0.65	4.15	4.44E-02
pTau217 + sex + age + InfTemp cortical thickness + InfTemp volume	0.68	11.10	1.23E-03
pTau217 + sex + age + InfTemp cortical thickness + InfTemp volume + inftemp PerpPD⁺	0.71	11.27	1.14E-03
pTau217 + sex + age + InfTemp cortical thickness + InfTemp volume + inftemp PerpPD⁺ + Dx	0.75	7.10	1.35E-03
Predictors	Adj_R^2	F_stat	p_value
pTau217	0.63	172.25	2.14E-23
pTau217 + sex	0.63	0.04	8.38E-01
pTau217 + sex + age	0.64	3.83	5.33E-02
pTau217 + sex + age + inftemp PerpPD⁺	0.70	20.01	2.12E-05
pTau217 + sex + age + inftemp PerpPD⁺ + Dx	0.74	8.53	3.94E-04
Braak 4 ROI	Adj_R^2	F_stat	p_value
Predictors			
pTau217	0.63	168.25	4.58E-23
pTau217 + sex	0.62	0.78	3.80E-01
pTau217 + sex + age	0.65	8.84	3.72E-03
pTau217 + sex + age + ADsig PerpPD⁺	0.75	38.81	1.24E-08
pTau217 + sex + age + ADsig PerpPD⁺ + Dx	0.78	7.47	9.76E-04

- Table 1 shows the adjusted R-squared values for progressively more complete linear models to predict inftemp tauPET, starting with pTau217 (R^2=63%), adding demographics, macrostructural atrophy (R^2=68%, p = 0.001), PerpPD⁺ (R^2=71%, p = 0.001) and diagnosis (R^2=74%, p = 0.001).
- p-value is the significance of the contribution for the newest component added to the model
- Even without macrostructural atrophy measures, PerpPD⁺ with pTau217 predicts tauPET in inferior temporal (R^2=70%, p= 2.12E-05) and in Braak-IV (R^2=75%, p= 1.24E-08).

Conclusions

- Diffusion MRI-derived PerpPD⁺ correlates robustly with regional and meta-regional tau PET
- PerpPD⁺ adds meaningful predictive value beyond plasma pTau217 and macrostructural atrophy, boosting explained variance and improving observed–predicted agreement.
- Multimodal models (blood + MRI volume/thickness + microstructure + Dx) provide the strongest performance.
- Next steps: Extend multimodal modeling with additional MRI contrasts readily available from clinical MRI, and prospective validation across larger cohorts.

Acknowledgments

The data used in preparation of this article were obtained from the Alzheimer's Disease Neuroimaging Initiative (ADNI) database (adni.loni.usc.edu). As such, the investigators within the ADNI contributed to the design and implementation of ADNI and/or provided data but did not participate in the analysis or writing of this report. A complete listing of ADNI investigators can be found at: http://adni.loni.usc.edu/wp-content/uploads/how_to_apply/ADNI_Acknowledgement_List.pdf

Disclosures

RD, GW, ZSS: Are employees of Johnson & Johnson and may hold stock and stock options.
GR, MT, PK, SC: Are employees of Oxford Brain Diagnostics Ltd. and may hold stock and stock options.

Funding

This study was funded by Johnson and Johnson

Alzheimer's Disease

Scan the QR code

The QR code is intended to provide scientific information for individual reference, and the information should not be altered or reproduced in any way.

Presented at the Alzheimer's Association International Conference (AAIC); July 12–15, 2026; London, United Kingdom

References:

La Joie R, Sci Transl Med. 2020 Jan 1;12(524):eaau5732; **Sanchez** JS,Sci Transl Med. 2021 Jan 20;13(577):eabc0655; **Weston** PS Alzheimers Res Ther. 2015 Jul 1;7(1):47; **Torso** M, et al J Prev Alzheimers Dis. 2022;9(4):769-779, **Ridgway** CTAD2022; **Torso** M, Alzheimers Dement. 2025 May;21(5):e70310; **Saad** ZS, Alzheimers Dement. 2026 Jun;22(6):e71573; **Therriault** J, Nat Aging. 2022 Jun;2(6):526-535.